

8-28-2012

Portable Bacterial Identification System Based on Elastic Light Scatter Patterns

Euiwon Bae

Dawei Ying

Donald Kramer

Valery Patsekin

Bartek Rajwa

See next page for additional authors

Follow this and additional works at: <http://docs.lib.purdue.edu/mcmppubs>

Recommended Citation

Bae, Euiwon; Ying, Dawei; Kramer, Donald; Patsekin, Valery; Rajwa, Bartek; Holdman, Cheryl; Sturgis, Jennifer; Davisson, Vincent J.; and Robinson, J Paul, "Portable Bacterial Identification System Based on Elastic Light Scatter Patterns" (2012). *Department of Medicinal Chemistry and Molecular Pharmacology Faculty Publications*. Paper 13.
<http://dx.doi.org/10.1186/1754-1611-6-12>

Authors

Euiwon Bae, Dawei Ying, Donald Kramer, Valery Patsekin, Bartek Rajwa, Cheryl Holdman, Jennifer Sturgis, Vincent J. Davisson, and J Paul Robinson

RESEARCH

Open Access

Portable bacterial identification system based on elastic light scatter patterns

Euiwon Bae¹, Dawei Ying², Donald Kramer³, Valery Patsekina⁴, Bartek Rajwa^{4,5}, Cheryl Holdman⁴, Jennifer Sturgis⁴, V Jo Davisson⁶ and J Paul Robinson^{4,5,7*}

Abstract

Background: Conventional diagnosis and identification of bacteria requires shipment of samples to a laboratory for genetic and biochemical analysis. This process can take days and imposes significant delay to action in situations where timely intervention can save lives and reduce associated costs. To enable faster response to an outbreak, a low-cost, small-footprint, portable microbial-identification instrument using forward scatterometry has been developed.

Results: This device, weighing 9 lb and measuring 12×6×10.5 in., utilizes elastic light scatter (ELS) patterns to accurately capture bacterial colony characteristics and delivers the classification results via wireless access. The overall system consists of two CCD cameras, one rotational and one translational stage, and a 635-nm laser diode. Various software algorithms such as Hough transform, 2-D geometric moments, and the traveling salesman problem (TSP) have been implemented to provide colony count and circularity, centering process, and minimized travel time among colonies.

Conclusions: Experiments were conducted with four bacteria genera using pure and mixed plate and as proof of principle a field test was conducted in four different locations where the average classification rate ranged between 95 and 100%.

Keywords: Portable bacterial identification, Forward scattering, Colony count, Automation

Background

Microbial identification is essential in various bioscience-related areas such as biosecurity, food safety, and monitoring and prevention of nosocomial infections. In general, three steps are needed to deliver correct identification of a species: sample acquisition/preparation, microbe detection, and microbe identification. Throughout the years, most effort in instrument development using optical technology has been focused on the development of a colony counter, which is essentially a detection device; further testing is required for identification. To identify and classify bacterial colonies, morphological methods, to

observe characteristics of the bacterial colony *via* visual inspection, are widely studied and applied [1-3]. Previous studies employed a number of image-processing tools [4-8] to realize the optical colony counting process, including distance transforms, adaptive thresholds, modified Hough transforms, etc. In recent years, prototype systems and software for simple and rapid automatic counting of bacterial colonies have also been developed. Liu et al. [9] adapted an imaging system originally developed for ELISPOT assays to count colonies automatically and used their system to measure serum bactericidal activity (SBA) in human sera. Later, Putman et al. [10] showed that automated colony counters can process images of plated bacterial colonies obtained with digital cameras or document scanners, so that small laboratories without a colony counter can send an image of a plate via the Internet and receive an accurate colony count from a remote laboratory that own a dedicated counting software. Recently, Clarke

* Correspondence: jpr@flowcyt.cyto.purdue.edu

⁴Dr. J. Paul Robinson Purdue University Cytometry Laboratory, Bindley Bioscience Center, Purdue University, 1203 West State Street, Discovery Park, West Lafayette, IN 47907, USA

⁵Department of Basic Medical Sciences, Purdue University, West Lafayette, IN 47907, USA

Full list of author information is available at the end of the article

et al. [11] presented a counting system equipped with a software called NICE (NIST's Integrated Colony Enumerator), which combines extended minima and threshold algorithms to locate colonies and distinguishes touching colonies. Chen and Zhang [12] proposed an automatic bacterial colony counter that can detect dish/plate regions, identify colonies, separate aggregated colonies, and report colony counts. In their paper, they used a typical morphology-based system, a one-class support vector machine (SVM) with radial basis function (RBF) as the colony classifier. However, in the proposed instrument, the incident laser beam is capable of extracting the microscopic morphological differences between bacterial colonies that are visually indistinguishable.

Most previous research focused only on counting the bacterial colony and consequently required further steps to identify the actual bacterial species. Our proposed instrument not only counts the colonies but also captures forward-scatter patterns to identify them; this is the crucial advantage over those systems already mentioned. The reported system embodies the design concept which employs Elastic Light Scatter (ESL) patterns for bacterial identification. Early work by Guo [13] and Banada et al. [14] inspired the development of a forward scatterometer-based detection and identification technology. The biophysical understanding of the elastic light scattering was reported by treating the individual bacterial colonies as biological spatial light modulators [15-17]. Briefly, the incoming wavefront of the light source interacts with the microscopic features of the bacterial colony and propagates to the imaging plane to provide a unique scatter pattern. No labeling agent is required to discriminate among different types of bacteria. The first reported forward scatterometer system required manual positioning of the incident beam and motion control to record the forward-scattering signatures, which is tedious, laborious, and inefficient. To increase the efficiency of the data acquisition process, Bae et al. [18] further developed a new version of the instruments that was fully automated.

In this report, we describe a portable forward scatterometer that is lighter in weight, is smaller in footprint, and provides wireless data transmission capability. These characteristics make the portable forward scatterometer a perfect instrument for field-deployable microbial identification as suggested by Robinson et al. [19]. To simulate this situation, a field test was conducted where ELS patterns captured remotely were electronically transmitted for classification and identification. Compared to the previous instrument, this system has a number of improvements. First, the instrument is designed with rotation-linear

movements rather than two linear movements, resulting in lighter weight and smaller instrument footprint. Second, several image-processing schemes have been added or improved (Hough transforms and R- θ centering algorithm). Third, wireless communication capability enabling access to the scatter-pattern database was incorporated to enable detection and identification from remote locations.

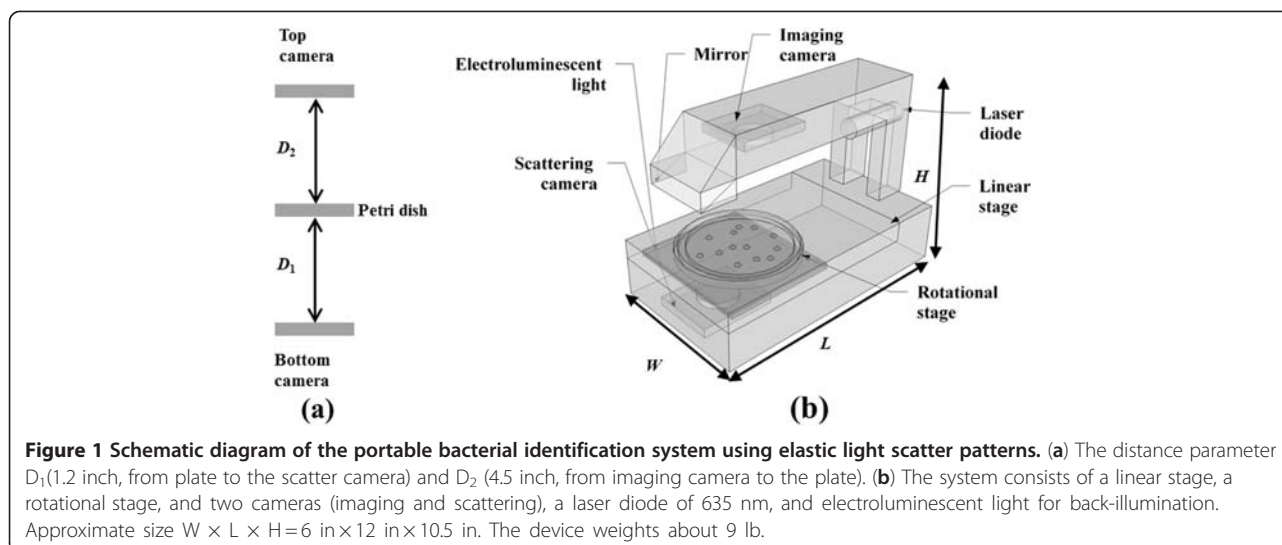
Results and discussions

Hardware

The proposed system is 12 (L) \times 6 (W) \times 10.5 (H) inches and weighs 9 lb. It consists of three distinct parts: a monochrome camera located right above the petri dish holder and used for colony counting and locating, a forward scatterometer, and a motorized stage that can rotate and translate the petri dish in the θ and R directions. The top camera (PL-B741U, PixeLINK, Ottawa, Canada) has 1280 \times 1024 resolution with a unit pixel size of 6.7 μ m. The camera is connected to a PC (Pentium 4, CPU 2.80 GHz, 1.00 Gb of RAM) via a standard USB 2.0 interface. An image of the petri dish is sent to the custom built analysis software that runs on a PC. The program coded in Visual C# 2008 (Microsoft, Seattle, WA, USA) is responsible for centering the stage, initializing the system, and counting and locating the bacterial colonies. An electroluminescent screen (PES-A6W parallel electrode system, Knema LLC, Shreveport, LA, USA) is placed under the petri dish to provide back illumination. The top imaging camera is equipped with an imaging lens ($f=8$ mm, M118FM08, Tamron, Saitama, Japan) with a viewing angle of 34 \times 25.6 $^\circ$ to cover the whole area of the plate within a given imaging distance (D_2 : 4.5 in.). The screen is turned on during the locating/counting phase to improve contrast. A schematic diagram of the proposed system is shown in Figure 1.

The forward scatterometer consists of a circular-beam laser module (Coherent Inc, Santa Clara, CA, USA), a 45 mirror, and a monochrome camera that is positioned just below the stage. The laser module has a wavelength of 635 nm and an output power of 0.95 mW. The camera used in the scatter module is the same as the colony imaging camera except for an added neutral-density filter (OD 2.5, Edmund Optics, Barrington, NJ) to prevent saturation of the CCD detector. The captured scatter patterns are imported to the colony-centering software, which performs automatic fine adjustment of the culture dish position to obtain circularly symmetric scatter signatures.

Motion control includes two stepper motors (PK243-01AA, Oriental Motor U.S.A. Corp, Torrance, CA, USA) driven by stepper-motor driver (MMD-17, Advanced



Micro Systems, Inc, Essex Junction, VT, USA); the drivers are controlled by a four-axis motion-control chip (UMX-26, Pro-Dex Inc, Beaverton, OR), which produces a half-duty cycle square-wave step pulse to control the motors under various operation speeds. Two motors control the movement of the stage in the R direction and rotation of the petri dish in the θ direction, respectively. Both stepper motors have a step angle of 1.8° . For rotation, the motor is attached to a gear with 24 teeth and drives a larger gear below the petri dish having 192 teeth, providing a resolution of 0.225° per step. Equivalently, for a petri dish with a diameter of 88 mm, the linear resolution is about 180 microns at the edge of the dish. For linear movement of the stage, the motor is connected to a lead screw having a pitch of 0.25 in. per revolution, resulting in a resolution of 0.00125 in., or $31.75 \mu\text{m}$ per step. The UMX-26 motion controller is also connected to a PC via a USB 2.0 interface, and is controlled by passing ASCII command strings to the chip. The controller provides a range of velocities from 0 to 1.044×10^6 step pulses per second and a range of accelerations from 0 to 8×10^6 pulses per second, where 400 pulses constitute a single revolution. A universal power supply (Smart-UPS 1400, American Power Conversion, W. Kingston, RI, USA) with 1400 VA capacity was used as a system power source when a field test was performed.

Software

As shown in Figure 2, a custom-built package was developed for automatic detection of scatter signatures. The software operates in of three phases: stage initialization, colony locating, and colony centering.

- 1) Stage initialization In the first phase, the stage is centered with respect to the imaging camera for acquisition of the whole petri dish image. Since the radius of the dish is fixed, it is possible to pick the circular outline of the dish rim in the image as a reference object. Application of the Hough transform [20-22] enables calculation of the distance between the center of the image and the reference outline.
- 2) Colony locating The colony counting and locating phase has five distinct steps: spatial filtering, colony separation, colony counting, colony location, and acquisition of morphometric characteristics. The spatial-filtering step resizes the image to 750×750 pixels, and assigns all HIGH (255) values to the area outside the petri dish. The colony-separation step binarizes the 8-bit image assigning 0 values to colonies and 1 values to the background. The binarization involves subtracting a pre-recorded background image from the actual plate image, and a segmentation process employing a region-growing algorithm to isolate the bacterial colonies [23,24]. The colony-locating step calculates the centroid of all the colonies and transforms Cartesian coordinates into polar coordinates. The final step calculates two morphometric parameters of the bacterial colonies: diameter and circularity. The diameter of a colony is expressed in pixels, and is computed using the following formula:

$$D = 2\sqrt{\left(\frac{A}{2\pi}\right)} \quad (1)$$

where A is the area of the colony in pixels, namely the total number of pixels found during

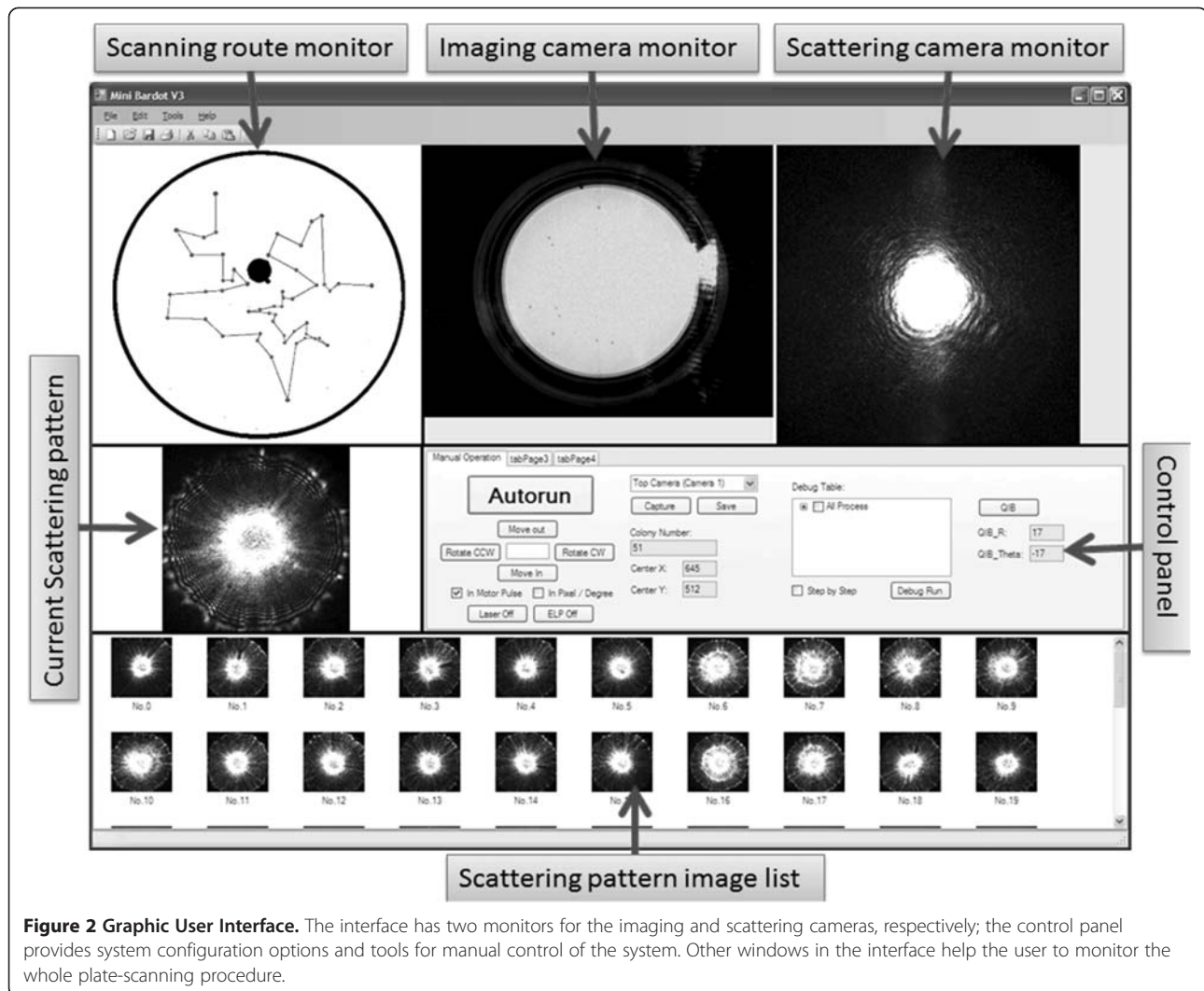


Figure 2 Graphic User Interface. The interface has two monitors for the imaging and scattering cameras, respectively; the control panel provides system configuration options and tools for manual control of the system. Other windows in the interface help the user to monitor the whole plate-scanning procedure.

colony segmentation. Meanwhile, the circularity is calculated as

$$C = \frac{4\pi A}{p^2} \quad (2)$$

where A is the area of the colony in pixels and p is the perimeter of the colony in pixels. The measurement of the perimeter is calculated as [25]:

$$\text{perimeter} = 0.948 \times n_{\text{even}} + 1.304 \times n_{\text{odd}} \quad (3)$$

where n_{even} is the number of even codes in the chain-code [26] representation of the colony edge and n_{odd} is the number of odd codes in the chain code. After locating the colony and obtaining the morphometric descriptors, the system performs a colony selection process, as colonies with diameters smaller than the predefined values or with low roundness values are excluded from the further

scanning. Non-circular colonies are generally formed by the intersection of two or more separate colonies.

3) Colony centering At the beginning of the colony-centering phase, optimum scanning trajectories through all selected colonies are computed by applying a generic algorithm to the equivalent traveling salesman problem. Bae et al. [18] showed that the generic algorithm provided efficient optimization results in a reasonable computation time. Following the given routine, the motion-control system moves the dish to the desired position, where the incident laser beam aims at the colony centroid location. However, since this centroid location is not identical to the centroid of the laser spot, macroscopic (coarse) adjustment is required to bring the two locations close to each other. Following this coarse movement, the software calculates the geometric centroid of the scatter pattern, which indicates the centeredness of the forward-scatter

images. The system automatically performs fine adjustment to align the measured centroid with the center of the laser beam until either the difference is smaller than the threshold or the maximum number of iterations [25] is reached. In the colony-separation step, background subtraction and thresholding is critical to ensure sound colony locating. To perform this in automatic fashion, the threshold to separate the colonies is given by an empirical formula:

$$\text{threshold} = 40 + \frac{1}{75}r + \frac{1}{6000}r^2 \quad (4)$$

where r is the distance of a pixel from the center of the image.

Elastic light scattering

ELS is defined as an optical measurement technique that utilizes the characteristics of the spatial distribution of the scattered light. ELS signal strength is very high compared to other spectroscopic and inelastic scattering techniques. By analyzing the ELS signal, it is possible to solve an inverse-scattering problem without any specific labeling reagent such as nucleic acid (DNA or RNA) or antibody probes, fluorophore molecules, or enzymes. The explanation of the ELS pattern differentiation originates from considering the bacterial colony as an optical amplitude/phase modulator [16,17]. When the photons from the laser interact with the micro structures of the colonies, the 2-D spatial distribution of the incoming

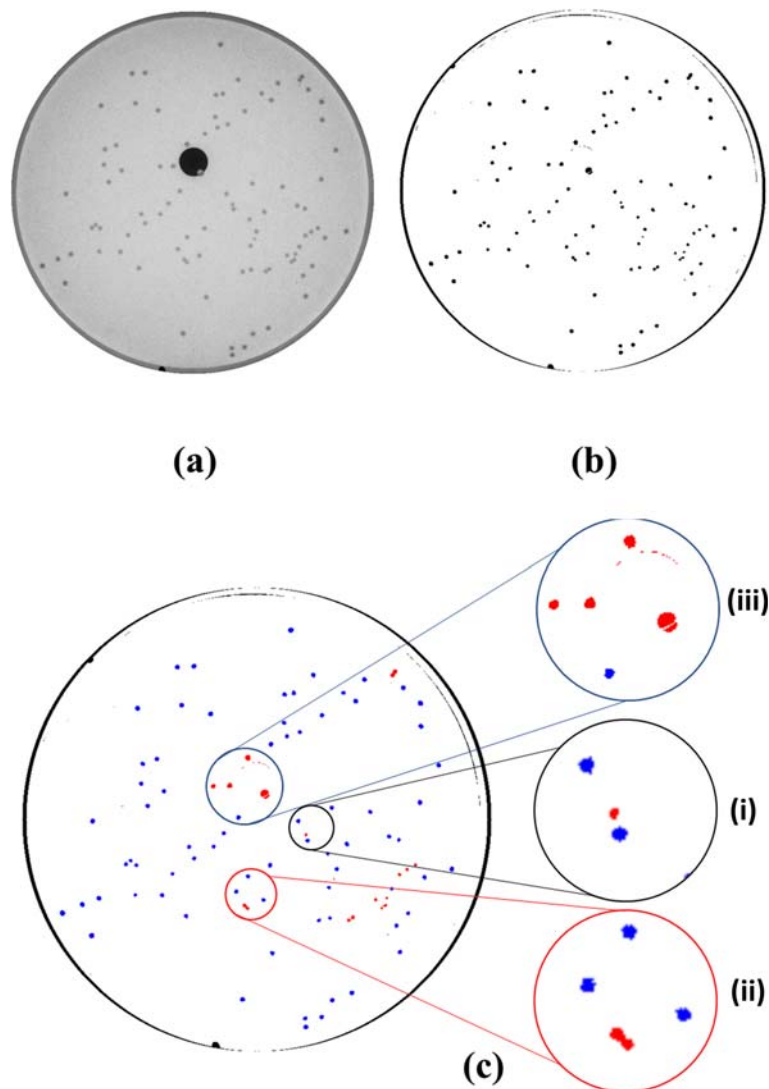


Figure 3 (a) Spatial filtering and colony counting. Raw plate image captured by the imaging camera. **(b)** Separation of colonies by subtracting the pre-saved background image and applying threshold. **(c)** Identification of colonies to be scanned by marking with blue color. **(i)** Colonies with too small or large diameters; **(ii)** colonies with low roundness values (indicating two or more intersecting colonies); **(iii)** colonies too close to the black hole in the raw plate image.

wavefront is modified depending on the morphological differences of the individual colony. Therefore, upon leaving the far side of the colonies, the departing wavefront is now encoded with different amplitude and phase modulation in 2-D space which can be theoretically modeled via the Huygens-Fresnel principle in rectangular coordinate [16,17]. When this disturbed wavefront is propagated to the imaging plane, the characteristic scattering pattern is generated via spatial interference.

Compared to optical microscopy, ELS provides high throughput results and correlates well with the three dimensional structures. In addition, ELS does not require any types of label or stain to interrogate biophysical characteristics. Microscopy provides the real image of the object whereas ELS provides a transformed image that requires a solution of inverse problem to actually image an object. However, if the purpose is to discriminate among minute morphological changes, ELS identifies the sample in a fast, accurate, and label-free way.

Pure and mixed plate experiments

Four different bacterial genera were scanned for single-species testing. Bacterial colonies were prepared as outlined in the material and methods section and three steps (stage initialization, colony locating, and colony centering) were performed automatically.

Figure 3 shows the result of colony-counting steps. After the raw image is captured from the camera (Figure 3(a)), background is subtracted before segmentation. Then, the system automatically marks the colonies that satisfy the selection criteria. These colonies are

queued into the trajectory optimization algorithm (Figure 3(c)). Colonies whose position lie close to the incident laser passage, or whose diameter is too small, or whose lack of circularity indicates a union of two colonies are eliminated from the scanning sequence. Finally, Figure 4 shows the centering mechanism in R- θ coordinates. Once the distance between colony centroid and laser center is known, rotational correction is performed to align the colony with the laser. Then a linear correction is performed to reduce the difference between the two centers to less than a pre-defined threshold. These coarse correction steps are followed by fine correction steps to provide circularly symmetric scatter patterns; an average of 6.67 fine adjustment steps per colony was required for 480 tested colonies. The typical average measurement speed for all three steps is approximately 2.7 colonies per minute; representative final scatter images are shown in Figure 5 for *L. innocua* F4248, *E. coli* stbl, *E. faecium*, and *S. aureus*.

Mixed plate experiments were then conducted. Among the four genera, three types of bacteria were selected; *L. innocua* F4248, *E. coli* stbl, and *E. faecium*. Mixed-plate experiments were performed in two steps. First we divided a single petri-dish in to three equal regions and inoculated the known bacterial genera. Figure 6(a) displays the three regions with different types of bacteria. Then we mixed all three genera and inoculated simultaneously without designating any boundary or regions. Nevertheless, the three genera were clearly separated by their distinctive ELS patterns (Figure 6(b)). Even though differentiation at genera level was shown, the

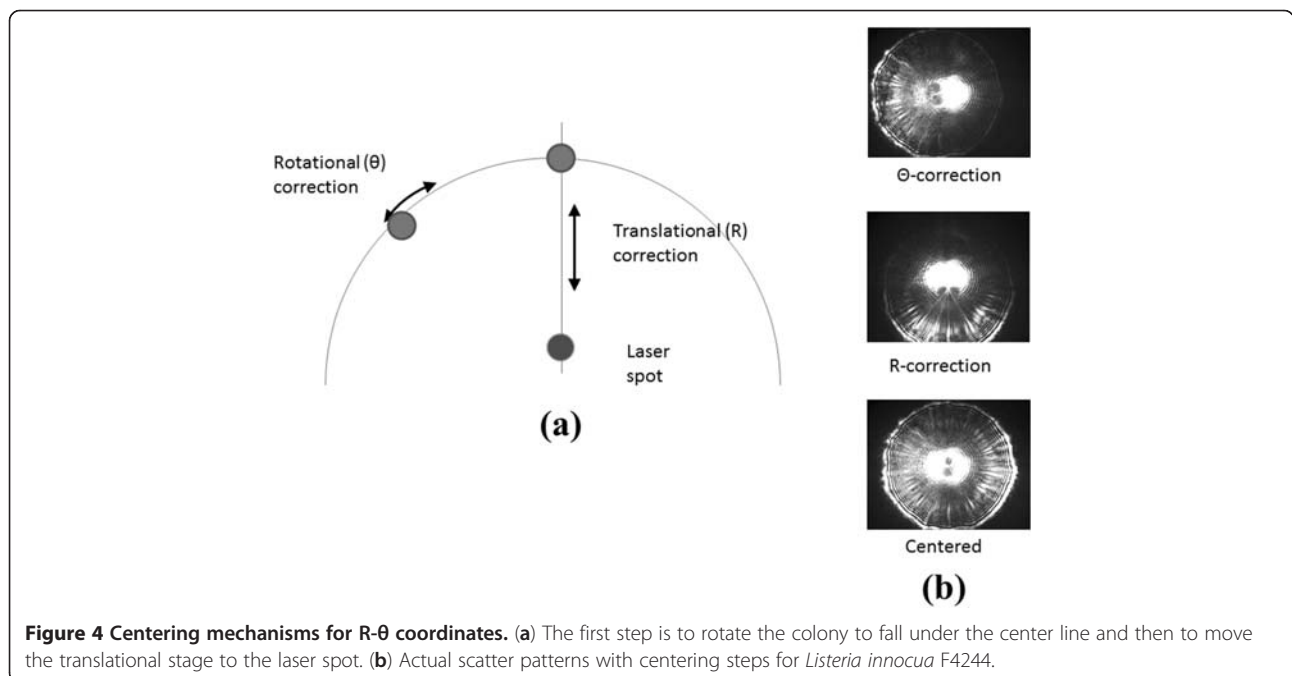


Figure 4 Centering mechanisms for R- θ coordinates. (a) The first step is to rotate the colony to fall under the center line and then to move the translational stage to the laser spot. (b) Actual scatter patterns with centering steps for *Listeria innocua* F4244.

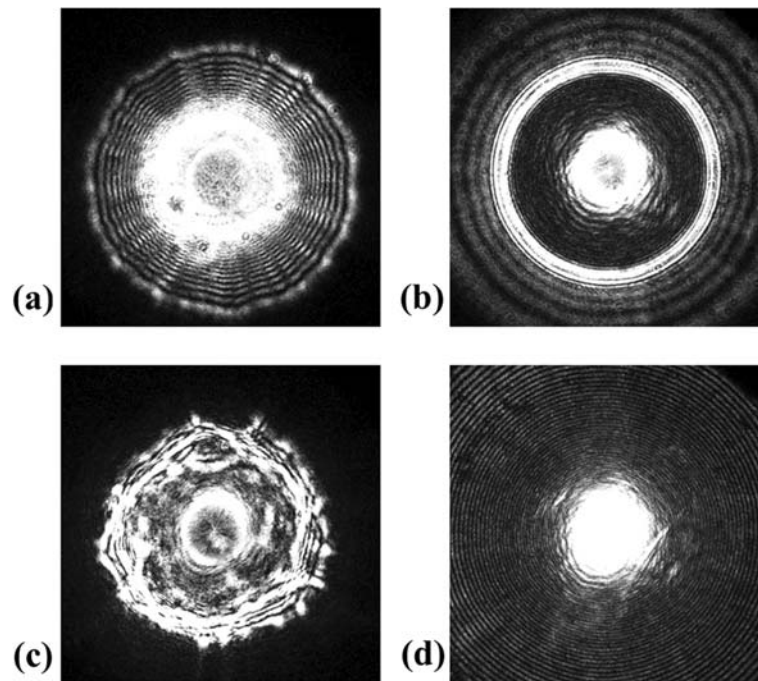


Figure 5 Representative scatter images for four different genera. (a) *L. innocua* F4244, (b) *E. faecium*, (c) *E. coli*, and (d) *S. aureus*.

discriminatory power of ELS has been proved to characterize at species level and in some cases, at strain level [27]. This was possible through combining the sensitivity of the ELS and quantitative classification software using Zernike and Haralick features

Comparison with forward scatterometer

Since the design aim of the portable instrument was operation as a field-deployable unit, we have compared the scatter patterns captured by the portable instrument and by the reference forward scatterometer located in the laboratory.

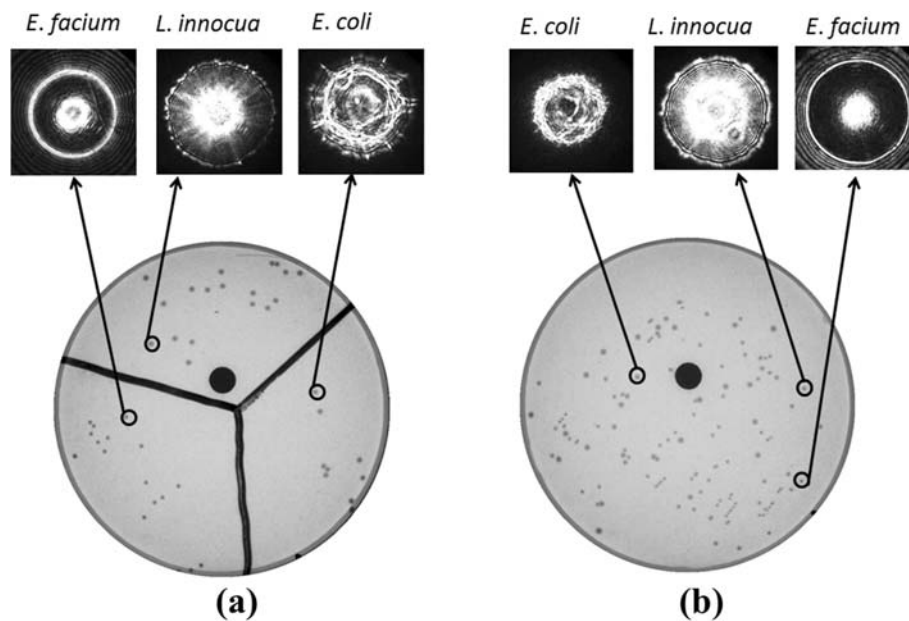


Figure 6 Petri-dish image of mixed plate experiment. (a) bacteria inoculated separately in different regions; (b) completely random inoculation.

Figure 7 shows the plate image from (a) the portable and (b) the reference instrument; the proposed system displays a black circle in the center area where the laser passes through. An important parameter that allows correlation of measurement between the two instruments is the colony diameter estimation, as it is used to select colonies for further analysis. Therefore, we compared the estimated diameters calculated from the images captured from both instruments and plotted the diameter correlation, as shown in Figure 7(c) (least square with $R^2 = 0.9191$). Most diameter values were close to each other; the error for the remainder was within 3-7%. In Figure 7, the maximum difference in percentage is 7.22%, and most pairs resulted in a difference of less than 3%. Since the image size of the 88-mm plate is 750×750 pixels, one pixel measures approximately 0.12 mm of physical length. Therefore, the typical diameter of a bacterial colony was 1-1.2 mm, or 10 pixels in one dimension; depending on the local noise level, a single-pixel difference in diameter measurement can cause the percentage error observed in the differences.

Field testing

Assuming a security threat from bioterrorism, field-deployable units can play an essential role in the process of identifying of the unknown agent. Since this device can be built for lower cost than reference instruments, it can be deployed in multiple locations to monitor and report any suspicious activity via ELS signatures of both clinical and food-borne bacteria. To emulate this scenario and provide a feasibility study of field-deployability, we operated the described instrument in a vehicle driven to four different locations near the Purdue University campus. Owing to safety regulations, only three genera (*L. innocua* F4248, *E. coli* stbl, and *E. faecium*) were prepared in the laboratory for the field testing. The representative scatter image and a list of measured species are shown in Figure 8 (a). Table 1 provides the GPS location (ThinkVantage GPS, Lenovo), the bacteria tested, and the final classification accuracy. Once the forward-scatter patterns were captured, the automated feature extraction following the process described previously was performed. The extracted

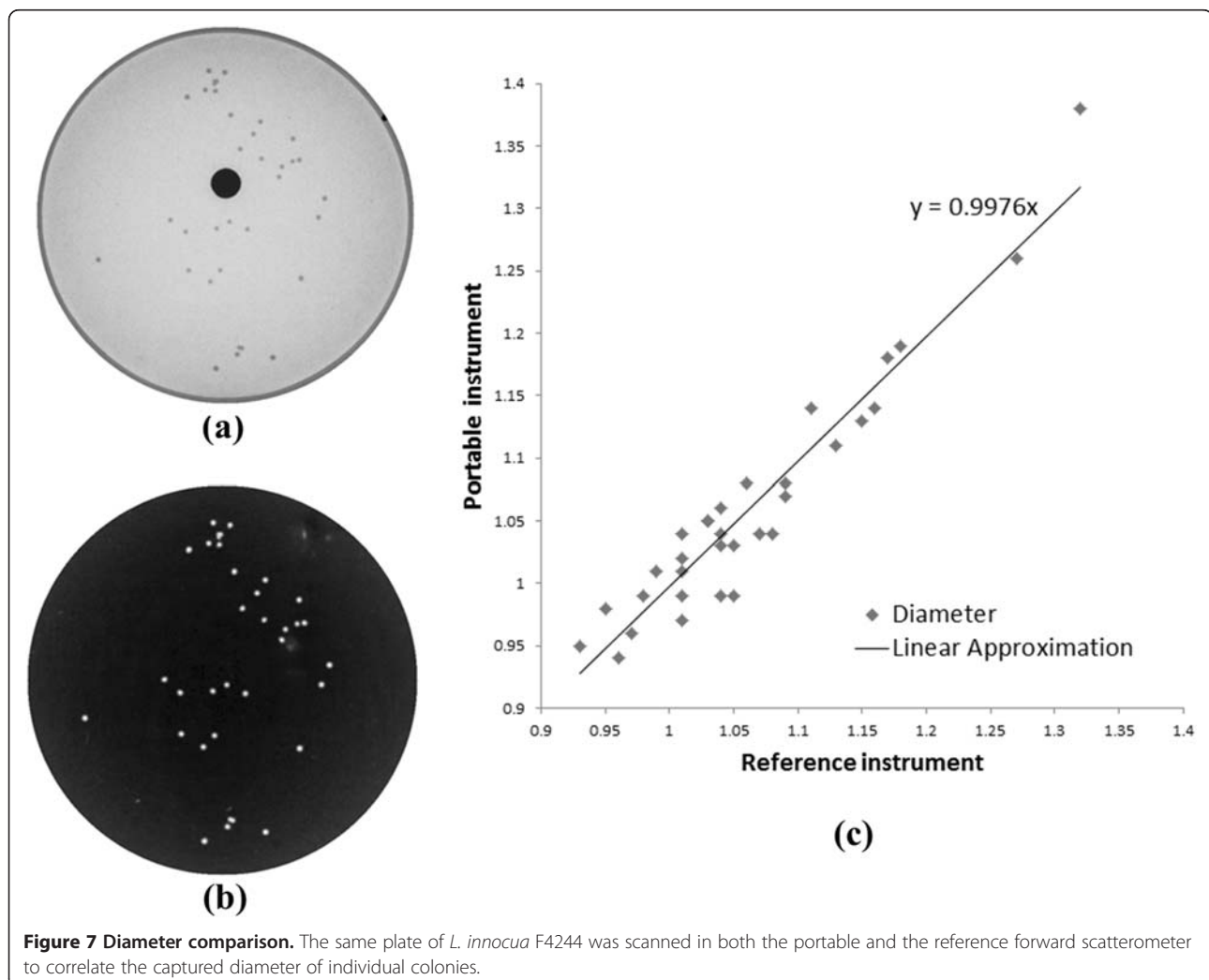
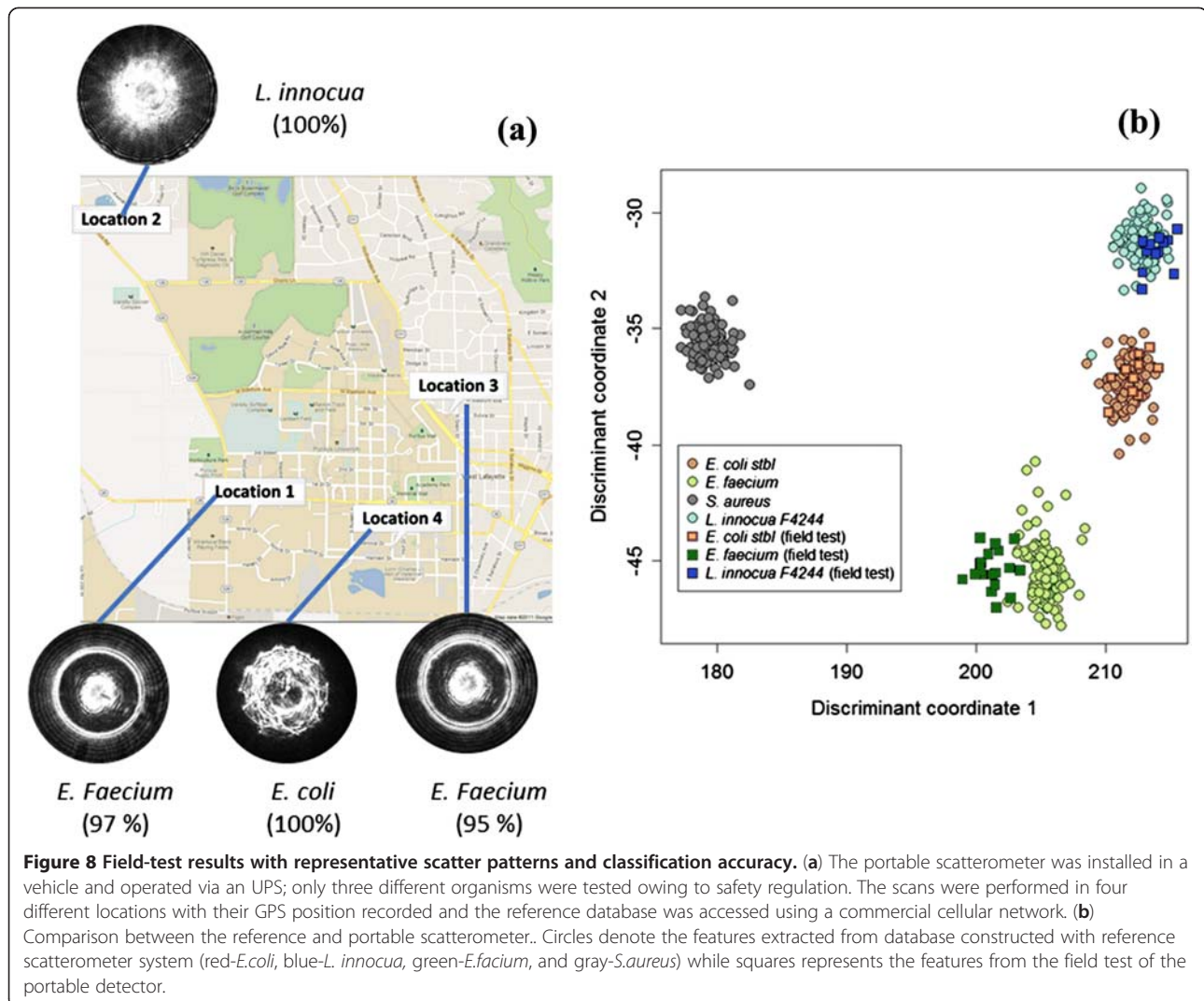


Figure 7 Diameter comparison. The same plate of *L. innocua* F4244 was scanned in both the portable and the reference forward scatterometer to correlate the captured diameter of individual colonies.



features were used by a remotely operated SVM classifier to automatically recognize the type of bacteria forming a particular colony [28,29]. The pattern database and the classifier were accessed through a commercial cellular network (AT&T HSDPA 3.6 Mbps); the overall classification accuracy for the three tested species was above 95%. Figure 8(b) shows the discriminant coordinates plot of randomly selected training colonies (characterized using the reference forward scatterometer), and projected scatter-patterns that were collected during the field test. Discriminant coordinates 1 and 2 are defined

as a linear combination of the Zernike and Haralick features that maximizes the distance between instances in different groups and minimizes the distance within groups. Although the actual classifier employed in our system is SVM-based, the 2-D plot of linear discriminate coordinates illustrates well the reproducibility and compatibility between the lab system, and the portable instrument. Circles represent the colonies characterized by scatter patterns measured with the regular lab system, while the squares represent data acquired using the portable device.

Table 1 Field-test data: GPS location, types of bacteria, and their classification accuracy

	GPS Coordinate	Bacterial species	No. of colonies	Mean accuracy
Location 1	Lat:40.422287 Long:-86.927704	<i>E. faecium</i>	21	97%
Location 2	Lat:40.44557 Long:-86.942497	<i>L. innocua</i>	25	100%
Location 3	Lat:40.430313 Long:-86.910759	<i>E. faecium</i>	18	95%
Location 4	Lat:40.420986 Long:-86.916092	<i>E. coli</i>	11	100%

The great advantage of the proposed instrument is shown by the field-testing results. Even though the experiment was performed locally around the campus, we can easily imagine the impact of using the portable device for resource-scarce areas. The screening result can be delivered wirelessly to the local instrument by accessing thousands of reference ELS images using feature extraction. The only drawback of the proposed system is that the system requires the bacterial colony to be grown on an agar medium. However, compared to the other reagents and expensive instruments needed for other types of screening, the petri-dishes and media can be considered as cost-effective consumables. In addition, numerous rapid methods require the plating of the bacteria anyway for final confirmation of the identification.

For hardware designs, since the UPS can provide 1400 VA of power and the consumption rate of the overall system is high, a single UPS can sustain about 15 min of continuous operation for the portable scatterometer and its accessories. This means that we can scan two plates of bacterial samples with an average number of 15-20 colonies per plate. In the future, both a higher-capacity power source and greater energy efficiency will be incorporated into the overall design of the system to maximize the measurement capability along with a modified optics to reduce the number of CCD cameras. Finally, the laser pointing stability is a critical issue when centering between the incoming laser and the colony center; measurements performed in a moving vehicle resulted in an increased number of centering steps or in poor scatter images. Therefore, all scanning and image acquisition were performed when the vehicle was parked.

Conclusions

A field-deployable bacterial identification system that uses elastic light scatter images has been introduced. The proposed device can provide more rapid identification of the source of an outbreak for resource-poor areas via wireless access capability to a central database, which can play an important role in constructing a national/international surveillance network. The portable device weighs 9 lb, is 12 × 6 × 10.5 inches, and is designed to access a scatter-fingerprint database using a commercial cellular wireless network. The hardware design includes a linear and rotational mechanism to provide a small footprint and incorporates various algorithms for colony locating and centering. Four representative bacterial genera, *L. innocua* F4248, *E. coli* stbl, *E. faecium*, and *S. aureus*, were used for single-species testing and comparison with the reference forward scatterometer for database compatibility. Finally, a field test was conducted at four different locations and resulted in classification rates of 95-100%.

Methods

Sample preparation

Four different bacterial genera were selected as representative samples: *Listeria innocua* F4248, *Escherichia coli* stbl, *Enterococcus faecium*, and *Staphylococcus aureus*. Trypticase soy agar (BD, catalog #211043) was used for sample preparation. 40 mg agar powder was suspended in 1 L Millipore water, boiled for 1 min, and allowed to cool. Twenty-five ml cooled agar was dispensed onto sterile 88-mm round petri dishes. Samples were serially diluted and 25 µl bacterial cultures was dispensed into the center of each petri dish. An L-shaped spreader (RPI Corp. #247660) was used to spread the bacterial dilution on the agar; the plate was then placed in a 37°C incubator.

Competing interests

The authors declare that they have no competing interests.

Authors' contributions

EB, DY, and DK contributed to the design of the hardware and programmed the operating software. VP and BR had developed and analyzed the SVM classification software; CH and JS provided the microbial samples for testing; VJD and JPR provided the guidelines for the overall project and contributed to the wireless database. All authors read and approved the final manuscript.

Acknowledgments

This research was supported through National Institute of Health Grant number 1R56AI089511-10.

Author details

¹School of Mechanical Engineering, Purdue University, West Lafayette, IN 47907, USA. ²School of Electrical and Computer Engineering, Purdue University, West Lafayette, IN 47907, USA. ³Visiting researcher, Cytometry Laboratory, Purdue University, West Lafayette, IN 47907, USA. ⁴Dr. J. Paul Robinson Purdue University Cytometry Laboratory, Bindley Bioscience Center, Purdue University, 1203 West State Street, Discovery Park, West Lafayette, IN 47907, USA. ⁵Department of Basic Medical Sciences, Purdue University, West Lafayette, IN 47907, USA. ⁶Department of Medicinal Chemistry and Molecular Pharmacology, Purdue University, West Lafayette, IN 47907, USA. ⁷Weldon School of Biomedical Engineering, Purdue University, West Lafayette, IN 47907, USA.

Received: 13 June 2012 Accepted: 23 August 2012

Published: 28 August 2012

References

1. Kawasaki K, Mochizuki A, Matsushita M, Umeda T, Shigesada N: **Modeling spatio-temporal patterns generated by *Bacillus subtilis***. *J Theor Biol* 1997, **188**:177-185.
2. Lacasta AM, Cantalapiedra IR, Auguet CE, Penaranda A, Ramirez-Piscina L: **Modeling of spatiotemporal patterns in bacterial colonies**. *Phys Rev E* 1999, **59**:7036-7041.
3. Mimura M, Sakaguchi H, Matsushita M: **Reaction-diffusion modelling of bacterial colony patterns**. *Physica A* 2000, **282**:283-303.
4. Barber PR, Vojnovic B, Kelly J, Mayes CR, Boulton P, Woodcock M, Joiner MC: **Automated counting of mammalian cell colonies**. *Phys Med Biol* 2001, **46**:63-76.
5. Bernard R, Kanduser M, Pernus F: **Model-based automated detection of mammalian cell colonies**. *Phys Med Biol* 2001, **46**:3061-3072.
6. Corkidi G, Diaz-Urbe R, Folch-Mallol JL, Nieto-Sotelo J: **COVASIAM: an image analysis method that allows detection of confluent microbial colonies and colonies of various sizes for automated counting**. *Appl Environ Microbiol* 1998, **64**:1400-1404.
7. Marotz J, Lubbert C, Eisenbeiss W: **Effective object recognition for automated counting of colonies in Petri dishes (automated colony counting)**. *Comput Meth Prog Bio* 2001, **66**:183-198.

8. Mukherjee DP, Pal A, Sarma SE, Majumder DD: **Bacterial colony counting using distance transform.** *Int J Biomed Comput* 1995, **38**:131–140.
9. Liu X, Wang S, Sendi L, Caulfield MJ: **High-throughput imaging of bacterial colonies grown on filter plates with application to serum bactericidal assays.** *J Immunol Methods* 2004, **292**:187–193.
10. Putman M, Burton R, Nahm MH: **Simplified method to automatically count bacterial colony forming unit.** *J Immunol Methods* 2005, **302**:99–102.
11. Clarke ML, Burton RL, Hill AN, Litorja M, Nahm MH, Hwang J: **Low-Cost, high-throughput, automated counting of bacterial colonies.** *Cytom Part A* 2010, **77A**:790–797.
12. Chen W-B, Zhang C: **An automated bacterial colony counting and classification system.** *Inform Syst Front* 2009, **11**:349–368.
13. Guo S: *Optical scattering for bacterial colony detection and characterization.* Purdue University: Masters degree; 2004.
14. Banada PP, Guo SL, Bayraktar B, Bae E, Rajwa B, Robinson JP, Hirleman ED, Bhunia AK: **Optical forward-scattering for detection of *Listeria monocytogenes* and other *Listeria* species.** *Biosens Bioelectron* 2007, **22**:1664–1671.
15. Bae E, Bai N, Aroonual A, Bhunia AK, Hirleman ED: **Label-free identification of bacterial microcolonies via elastic scattering.** *Biotechnol Bioeng* 2011, **108**:637–644.
16. Bae E, Bai N, Aroonual A, Robinson JP, Bhunia AK, Hirleman ED: **Modeling light propagation through bacterial colonies and its correlation with forward scattering patterns.** *J Biomed Opt* 2010, **15**:019004.
17. Bae E, Banada PP, Huff K, Bhunia AK, Robinson JP, Hirleman ED: **Biophysical modeling of forward scattering from bacterial colonies using scalar diffraction theory.** *Appl Opt* 2007, **46**:3639–3648.
18. Bae E, Aroonual A, Bhunia AK, Robinson JP, Hirleman ED: **System automation for a bacterial colony detection and identification instrument via forward scattering.** *Meas Sci Technol* 2009, **20**:015082.
19. Robinson JP, Rajwa BP, Dunder MM, Bae E, Patsekina V, Hirleman ED, Roumani A, Bhunia AK, Dietz JE, Davison VJ, Thomas JG: **A distributed national network for label-free rapid identification of emerging pathogens.** In *Chemical, Biological, Radiological, Nuclear, and Explosives (CBRNE) Sensing XII. Volume 8018. 1 edition.* Edited by Fountain III AW, Gardner PJ. Orlando: SPIE; 2011:80180C–80186C. Proceedings of SPIE.
20. Ballard DH: **Generalizing the Hough transform to detect arbitrary shapes.** *Pattern Recognition* 1981, **13**:111–122.
21. Hough PVC: *A method and means for recognizing complex patterns.* USA: US3069654; 1962.
22. Leavers VF: **Which Hough transform?** *CVGIP: Image Understanding* 1993, **58**:250–264.
23. Mancas M, Gosselin B, Macq B: **Segmentation using a region growing thresholding.** In *Image Processing: Algorithms and Systems IV. Volume 5672.* Edited by EK O.: Proceedings of the Society of Photo-Optical Instrumentation Engineers (SPIE); 2005:388–398.
24. Pham DL, Xu CY, Prince JL: **Current methods in medical image segmentation.** *Annu Rev Biomed Eng* 2000, **2**:315–337.
25. Proffitt D, Rosen D: **Metrication errors and coding efficiency of chain-encoding schemes for the representation of lines and edges.** *Comput Vision Graph* 1979, **10**:318–332.
26. Freeman H: **On the encoding of arbitrary geometric configurations.** *Electronic Computers, IRE Transactions on* 1961, **EC-10**:260–268.
27. Banada PP, Huff K, Bae E, Rajwa B, Aroonual A, Bayraktar B, Adil A, Robinson JP, Hirleman ED, Bhunia AK: **Label-free detection of multiple bacterial pathogens using light-scattering sensor.** *Biosens Bioelectron* 2009, **24**:1685–1692.
28. Bayraktar B, Banada PP, Hirleman ED, Bhunia AK, Robinson JP, Rajwa B: **Feature extraction from light-scatter patterns of *Listeria* colonies for identification and classification.** *J Biomed Opt* 2006, **11**:34006.
29. Rajwa B, Dunder MM, Akova F, Bettasso A, Patsekina V, Hirleman ED, Bhunia AK, Robinson JP: **Discovering the unknown: detection of emerging pathogens using a label-free light-scattering system.** *Cytom Part A* 2010, **77A**:1103–1112.

doi:10.1186/1754-1611-6-12

Cite this article as: Bae et al.: Portable bacterial identification system based on elastic light scatter patterns. *Journal of Biological Engineering* 2012 **6**:12.

Submit your next manuscript to BioMed Central and take full advantage of:

- Convenient online submission
- Thorough peer review
- No space constraints or color figure charges
- Immediate publication on acceptance
- Inclusion in PubMed, CAS, Scopus and Google Scholar
- Research which is freely available for redistribution

Submit your manuscript at
www.biomedcentral.com/submit

